JARQ 52 (3), 197-204 (2018) https://www.jircas.go.jp

REVIEW

Identification of Paddy Rice Areas Using SAR: Some Case Studies in Japan

Naoki ISHITSUKA*

Institute for Agro-Environmental Sciences, NARO (Tsukuba, Ibaraki 305-8604, Japan)

Abstract

Rice is a staple food across Southeast Asia. However, not all Southeast Asian countries are self-sufficient in rice production, and there is significant import-export trade. Foodstuffs and agricultural products have significant environmental impacts, which in the case of rice include demand for water, as rice farming is water-intensive. It is therefore important to understand the dynamics of rice paddy fields. Satellite remote sensing is one of the most effective methods of grasping the area and distribution of farmland. However, East and Southeast Asia have distinct rainy seasons, making clear skies rare and data collection difficult during the growing period in visible and near infrared image data. Synthetic Aperture Radar (SAR) is unaffected by cloud cover, and can thus offer a method of monitoring agricultural areas. This paper introduces a method of identifying paddy rice planted areas using SAR and some case studies in Japan.

Discipline: Information technology
Additional key words: remote sensing, satellite, water

Introduction

Rice is a staple food across Southeast Asia, which is a center of rice production and consumption. Rice also plays a central role in the life and culture of the region, forming the basis of festivals and the annual calendar. However, not all Southeast Asian countries are self-sufficient in rice production, and there is significant import-export trade. Foodstuffs and agricultural products have significant environmental impacts, which in the case of rice include demand for water, as rice farming is water-intensive. A recent suggestion known as "virtual water" proposes that the water required for the production of a product be bought and sold along with the product itself. The water demand for rice production is 3,600 m^3 t/kg, while that for wheat and corn production is 2,000 m^3 t/kg and 1,900 m^3 t/kg, respectively (estimates based only on the edible part from cultivation in Japan (Oki et al. 2004)). It is clear that rice needs significantly more water than the other main food grains. It is thus important to understand the dynamics of rice paddy cultivation.

Satellite remote sensing is one of the most effective methods of grasping the area and distribution of farmland. Accurate estimation of rice acreage has been conducted using Landsat TM data (e.g., Okamoto et al. 1996). However, East and Southeast Asia have distinct rainy seasons, making clear skies rare and data collection difficult during the growing period in visible and near infrared image data. Synthetic Aperture Radar (SAR) is unaffected by cloud cover, and can therefore offer a method of monitoring agricultural areas. The idea of using SAR for determining a rice paddy area is not a recent one. For example, there is paper that reported the monitoring of rice fields using ERS-1 data (Kurosu et al. 1995, Toan et al. 1997). Given that most rice fields are small, the spatial resolution of SAR is insufficient to allow accurate measurement, as a rice paddy is often mixed with fields growing other crops. However, the spatial resolution of SAR is improving along with the additional use of polarization. This paper introduces a method of identifying paddy rice planted areas using SAR and some case studies in Japan.

*Corresponding author: e-mail isituka@affrc.go.jp
Received 31 March 2017; 26 September 2017.

Methodology

Paddy fields are waterlogged during the rice-transplanting period. SAR is a microwave-based active sensor that transmits microwaves to the target and then records the backscatter. The microwaves undergo specular reflection when encountering water or a smooth ground surface. This reduces the backscatter coefficient of SAR in a water-covered area, providing an estimation method for a rice paddy area, as the backscatter coefficient is very low just after transplanting.

Figure 1 shows the surface cycle of the fields. The paddy is waterlogged during the transplanting period. Just after transplanting, the rice plants are very small and the microwaves can penetrate the plant bodies, giving the same reflectivity as that of a body of water. During the growing period, the microwaves are unable to penetrate the rice bodies, causing the backscatter coefficient to increase. When other crops are planted in paddy fields, the crops are flooded with water in neither the transplanting period nor the growing period, though some rice production control fields are waterlogged to protect against weed growth. Identification of the rice-planted fields therefore requires two scenes of SAR data: the detection of areas of water, followed by no detection of water. Fields that exhibit this pattern are assumed to be paddies planted with rice.

Case studies

Case 1: Determination of paddy rice planted area using SAR images (Ishitsuka 2003)

The area of study was the Saga Plain in Kyushu in southeast Japan. The Saga Plain extends across the prefectures of Saga and Fukuoka. The annual average temperature is 16ºC, with annual rainfall of 1,836 mm. Rice is the main crop in summer, and wheat in winter. In this study, two RADARSAT images were acquired using the same S2 mode on July 2nd and 27th in 2000. Path images were calculated by the EarthView Advanced Precision Processor (APP) from raw SAR signal data. Ground control points were added onto the satellite image, and geo-rectified to the UTM coordinates using the 1:25 000 digital map of the Geographical Survey Institute of Japan (GSI). A 3 × 3 sigma filter was then applied to the images for reducing the speckle noise.

The July 2nd image was taken at the end of the rice-transplanting period, when the backscatter coefficient of RADARSAT in the rice planting fields was very small. The July 27th image was taken in the rice growing period, when the backscatter coefficient increased (Fig. 2).

Dark areas were extracted from each image by thresholds and assumed to represent water areas. The dark areas extracted from the July 2nd RADARSAT image comprised bodies of water, paddy fields, and areas of flat ground, where the smooth surface produced specular reflection. The dark areas extracted from the July 27th RADARSAT image comprised of bodies of water, unplanted paddies, and areas of flat ground. The one-month period that had elapsed since the transplanting of rice was sufficient to detectably increase the backscatter coefficient of the data from RADARSAT, which uses C-band microwaves. Areas of planted paddies increased in brightness, whereas unplanted areas remained dark. An unplanted paddy is normally kept waterlogged to control weed growth.

Planted paddy fields were identified by subtracting the July 27th data from the July 2nd data. The vector boundaries of cities, towns, and villages were taken from the 1:25,000 digital map, allowing the planted paddy area of each municipality to be determined and compared with the published statistical value.

Figure 3 shows the results of applying this method to the two RADARSAT images. The ratio of extracted area to published statistical area was 97.8%, which is satisfactory. However, the ratio of extracted area by municipality was between 25.8% and 120.9%, with a standard deviation of 19.2.

The ratio was lower for municipalities in mountainous regions than for those on the plains. This is reflected by the influence of foreshortening and layover phenomena, which caused positioning errors in both images. It was

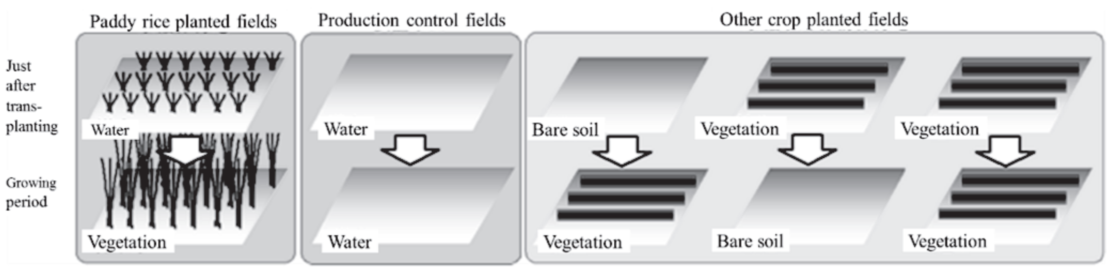

Fig. 1. Variety of surface change in the fields

thus necessary to apply geometrical correction using a digital elevation model (DEM). Figure 4 shows the result of applying geometrical correction using the 50 m DEM of GSI. The ratio of aggregate estimation rose to 101.6%, and that at the municipality level increased to between 53.8% and 122.0%, with a standard deviation of 13.1.

Case 2: Determination of paddy rice planted area using SAR images with GIS polygon (Ministry of Agriculture, Forestry and Fisheries 2010)

As the Japanese people's diet has improved and diversified, the consumption of rice has declined and so has the role of rice as the mainstay crop in Japanese agriculture. However, rice yields have increased year by year thanks to improvements in breeding and agricultural techniques. The difference between supply and demand has thus widened, and since the 1970s, the Japanese government has pursued a policy of reducing rice acreage and controlling the production of rice, in order to reduce the surplus. The acreage has been reduced by more than 30%, and the area is now somewhat above 1,000,000 ha. Large rice paddy areas have been converted to grow upland crops such as wheat, barley, and soybean, or developed for housing.

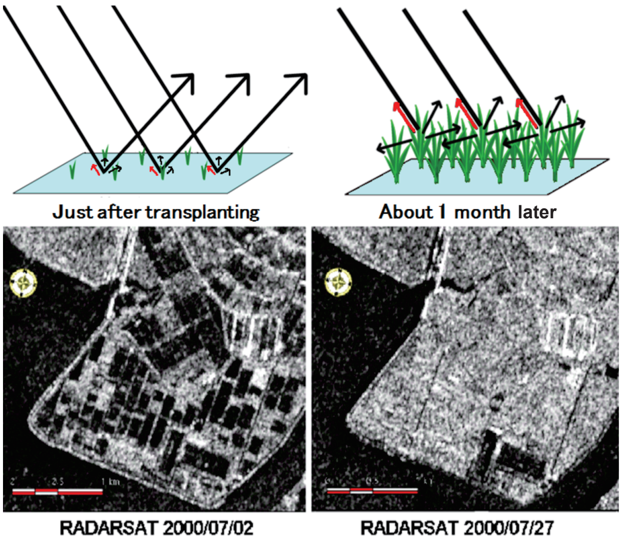

Fig. 2. Change of backscatter in paddy rice planted fields
Example of the Saga Plain in Kyushu in southeast Japan. The backscatter coefficient of the paddy fields was very small in the July 2nd image. The backscatter coefficient of rice planted area increased in the July 27th image.

Every year, the statistics department of the Ministry of Agriculture, Forestry, and Fisheries (MAFF) collects data on rice-planted areas and rice yields to support the production control program. The planted area of paddies is now calculated using a statistical method based on a physical survey of about 38,000 fields throughout Japan. This method is expensive and time consuming, and manpower constraints and personnel costs limit its accuracy at the field level.

The Japanese government is therefore seeking alternative, low-cost methods. One possible solution is remote sensing. However, the annual statistical values must be accurate. To tackle the problem of cloud cover blocking optical sensor observations, measurement methods using SAR are being developed.

Between 2009 and 2010, the statistics department of MAFF carried out one such project to develop the application of satellite imagery to the measurement of rice-planted areas in Japan. In this project, the determination method was improved to combine SAR data with GIS data, which are the parcels polygon data of fields. First, the mean value of the backscatter coefficients was calculated for each field parcel (Fig. 5).

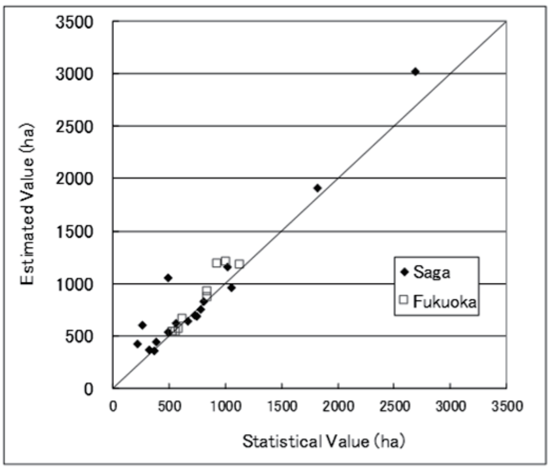

Fig. 3. Comparison of statistical area and estimated area

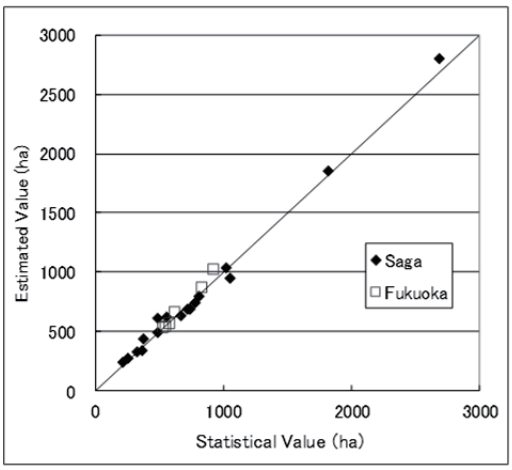

Fig. 4. Comparison of statistical area and estimated area with geometric correction using DEM

Next, the parcels were separated into waterlogged and non-waterlogged using these thresholds, which were set using the discriminant analysis method.

In 2009, the project was carried out using TerraSAR-X, RADARSAT-2 and ALOS/PALSAR (Table 1). Ground truth data for use as validation were collected from thousands of fields in each of the cities, giving a total of about 25,000 fields and a total area coverage of about 3,100 ha.

The average accuracy (overall accuracy) of TerraSAR-X was about 93%, with a range from 88% to 99% for different cities. The average accuracy of RADARSAT-2 was about 92%, with a range from 88% to 99% for different cities. The average accuracy of ALOS/PALSAR was about 72%, with a range from 46% to 81% for different cities. These results on the accuracy of ALOS/PALSAR were rather low compared to the results using RADARSAT-2 or TerraSAR-X. A major cause of this low accuracy was thought to be the spatial resolution of ALOS/PALSAR. Moreover, such low accuracy affects the timing of the observations. It is difficult for ALOS/PALSAR to observe optimal timing as the revisit time of ALOS/PALSAR is 46 days given the same incident angle; in contrast, it is 24 days for RADARSAT-2 and 11 days for TerraSAR-X.

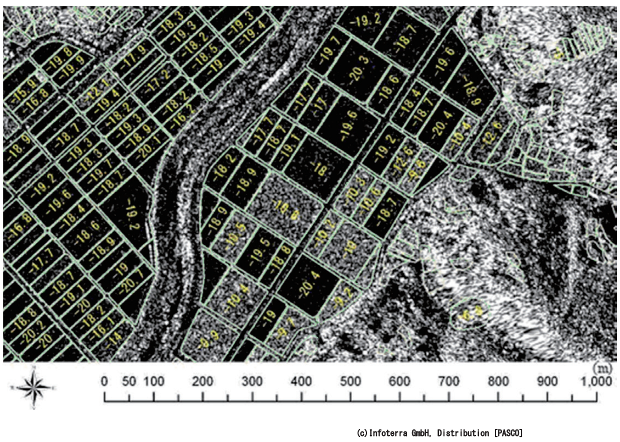

Fig. 5. Difference between waterlogged fields and non-waterlogged fields
The background image is TerraSAR-X. Polygons are field parcels and the number of parcels is the mean of backscatter coefficients.

Case 3: Detecting of waterlogged paddy fields for a wide area; huge number of paddy fields (Ishitsuka 2015)

An accident at the Fukushima Dai-ichi Nuclear Power Station run by the Tokyo Electric Power Company (Fukushima I) was precipitated by the Great East Japan earthquake and subsequent tsunami that struck on March 11th, 2011. This accident captured the world's attention amid concerns about the radionuclides released into the environment. This study attempted to assess the environmental state of the farmland in Fukushima and neighboring prefectures in 2011, using satellite remote sensing to better understand the radioactive contamination of the farmland.

Four images from RADARSAT-2 data were used. These observations were made on June 7th, 9th, 19th and 26th via the Wide Fine mode with a center incident angle of 31.27°, a spatial resolution of 10.2-8.2 m by 7.7 m, and using HH polarization. Agricultural parcel polygon GIS data were also used. The satellite data were preprocessed and then the mean values of the backscatter coefficients were calculated for every agricultural parcel in the study area. The threshold was set from the histogram of backscatter coefficients. Agricultural parcels were masked on a land use map provided by the National Institute for Agro-Environmental Sciences (NIAES). The map could only extract nominal paddy fields. Each nominal paddy field was classified as waterlogged or non-waterlogged using the threshold.

The waterlogging status of paddy fields was distinguished and mapped at approximately 3,200,000 parcels over the prefectures of Fukushima, Ibaraki, Tochigi, and Gunma (Fig. 6). The overall accuracy of the map was evaluated at 77.05% and producer accuracy at 89.6% using ground truth data from 2,597 fields. This was sufficiently accurate for the intended purpose. The results formed one of the inputs for creating a radioactive substance pollution density distribution map of the farmland soil (Takata et al. 2014).

Table 1. Satellite image data used for determination of rice paddy fields

Satellite	Band (wavelength)	Mode	Spatial resolution	Number of observation	Revisit time
TerraSAR-X	X (3.1cm)	StripMap	3 m	59	11 days
RADARSAT-2	C (5.6cm)	MultilookFine	8 m	85	24 days
ALOS/PALSAR	L (23.6cm)	FBS	10 m	34	46 days

Wavelengths in this table are the center wavelength of each sensor. The IEEE Standard defines the following: X band: 2.5-3.75 cm, C band: 3.75-7.5 cm, L band: 15-30 cm. The frequency and band name differ by definition, such as in the NATO Standard.

Case 4: Monitoring the recovery of rice fields from tsunami; Temporal change (Ishitsuka 2013, 2014)

On March 11th, 2011, a major earthquake caused enormous damage in a wide area of Northeastern Japan. Many farmlands also suffered damage, and the Pacific coast was hit by a massive tsunami. This study attempted to evaluate the recovery process of rice paddy fields there.

The paddy fields were waterlogged in the early growth period. Therefore, waterlogging was regarded as indicating cultivation activity. SAR can detect a water surface through microwave specula reflection. This allowed the detection of a paddy in which rice cultivation was conducted each year. The results were used to evaluate the recovery progress. SAR observations were carried out every year following the tsunami by using RADARSAT-2 (2011), TerraSAR-X (2012), and Cosmo-SkyMed (2013). This yielded the images listed in Table 2.

Figure 7 shows the SAR images of the tsunami-damaged area, with the dark area spreading year by year. This shows the extent to which the paddy fields had recovered from the tsunami damage, and expansion of the recovered area. However, the earthquake caused the ground level to subside by about 30-120 cm along the Pacific coast area of Miyagi Prefecture. This formed ponds (produced by high tides) that are not marked on existing maps, a rise in the water level, or poor drainage. These ponds influenced the accuracy of detection.

These analyses led the government to conclude that SAR is a useful technique for monitoring the recovery of

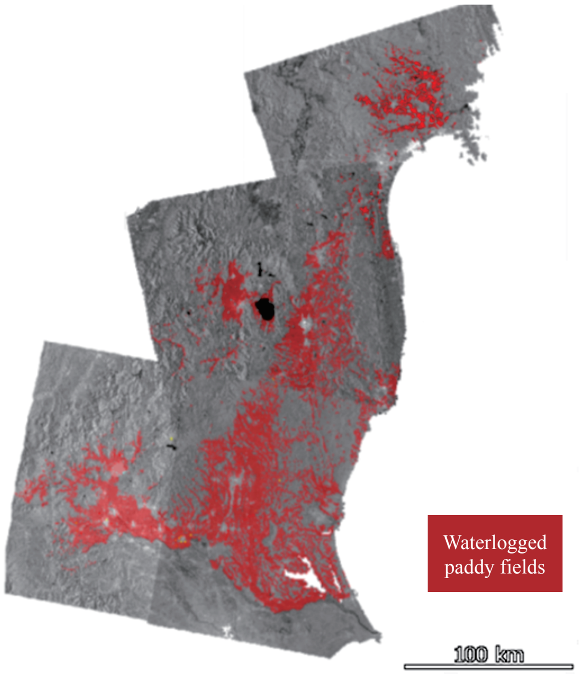

Fig. 6. Map of waterlogged paddy fields in 2011

Table 2. Satellite image data used for monitoring the recovery of rice fields from tsunami damage

Satellite	Date	Band (wavelength)	Mode	Spatial resolution
RADARSAT-2	7-Jun-2011	C (5.6cm)	WideFine	10.2-8.2 m x 7.7 m
TerraSAR-X	30-May-2012	X (3.1cm)	StripMap	3 m
Cosmo-SkyMed	22-May-2013	X (4.6cm)	StripMap	3 m

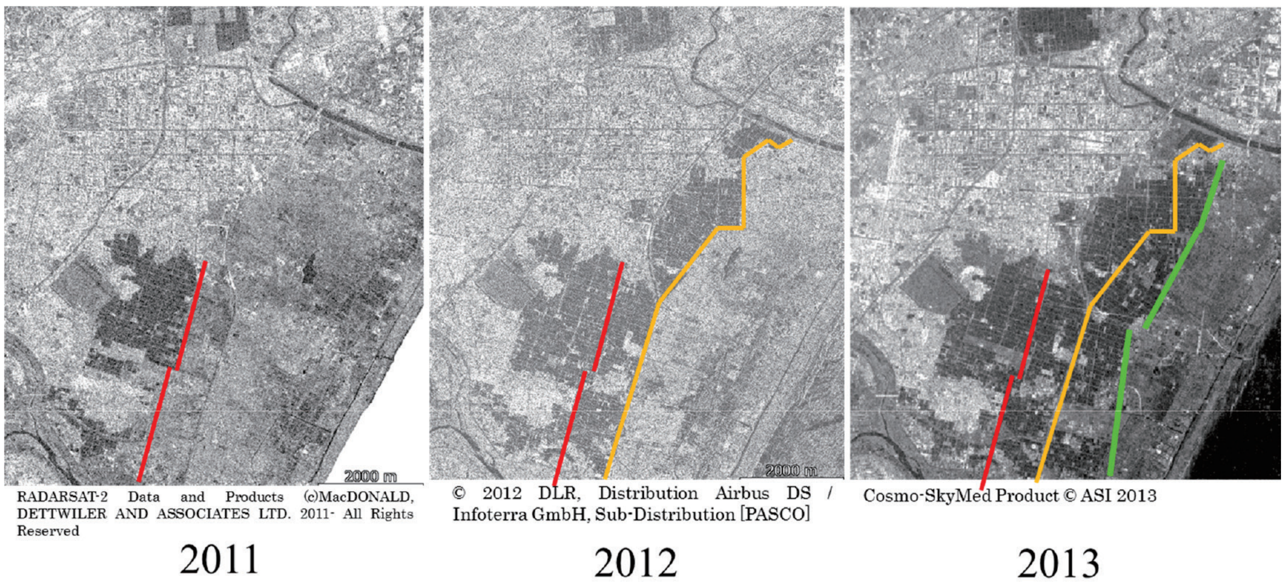

Fig. 7. Monitoring of paddy rice fields recovering from tsunami damage
(Recovery front line: red in 2011, yellow in 2012, green in 2013)

rice fields.

Case 5: Polarimetric analysis (Ishitsuka 2011)

SAR is an emerging technology for observing multi polarimetric data. Polarization is an index used to describe the characteristics of electromagnetic waves and express the orientation of the electric field. When the electric field is vertical, the electromagnetic wave is said to be vertically polarized. When the electric field is horizontal, the electromagnetic wave is said to be horizontally polarized. Elliptically and circularly polarized waves are formed by combining the vertically and horizontally polarized waves (JAXA EORC HP). PALSAR is the first satellite-borne L-band synthetic aperture radar capable of fully polarimetric observation, and can transmit and receive both horizontally and vertically polarized signals. The combined polarization radar image can therefore be HH (horizontal transmitting, horizontal receiving), VV (vertical transmitting, vertical receiving), HV (horizontal transmitting, vertical receiving), or VH (vertical transmitting, horizontal receiving).

This case study was conducted in Tsukuba (36° 01' 57" N, 140° 04' 38" E) in Ibaraki Prefecture, Japan. In this region, paddy fields start to become waterlogged in late April, with transplantation carried out in early May. Harvesting is usually done in mid-September. The fully polarimetric PALSAR data were observed on August 24^{th} and October 9^{th}, 2008. In August, rice grows in the paddy fields. However, some paddy fields are planted with other crops, such as soybeans. In October, the rice has been already harvested, and most rice-planted fields are covered with residue, although the soybeans have yet to be harvested.

DEM data at 10 m provided by GSI were used for orthorectification. Polygon vector data for each paddy field parcel were created using head-up digitizing of the aerial orthophoto. In 2008, the planted crops were checked, revealing that 262 paddy fields were planted with rice, while 76 were planted with wheat or soybeans. Fully polarimetric (PLR) PALSAR data (Level 1.1) were analyzed using "PolSARpro" software (ESA). The results were compared with the ground survey data on planted crops, in order to analyze the scatter characteristics and evaluate the accuracy of classification.

Figure 8 shows images of the double-bounce scatter component using the three-component decomposition analysis proposed by Freeman and Durden (Freeman & Durden 1998) with a 2 x 2 window size. In the August image, a double-bounce scatter component appeared in the rice-planted paddy fields. In contrast, the double-bounce scatter component was less in the October 9^{th} image (area circled by the solid line). The author considers that this double bounce was caused by the water and rice stems.

It was difficult to separate rice-planted paddy fields from paddy fields planted with other crops using unsupervised classification (K-means method) with four-polarization σ^0 data. The author therefore applied the K-means unsupervised classification method with the Dbl, Odd and Vol components from Freeman and Durden's three-component decomposition analysis. The author attempted classification using all combinations of the three components. As a result, an accuracy of 58.8% was achieved in the detection of rice-planted paddy fields when using the Dbl and Odd components. This was close to the accuracy reported by McNairn et al. (2009) when using single-scene PLR data. This was judged as a good

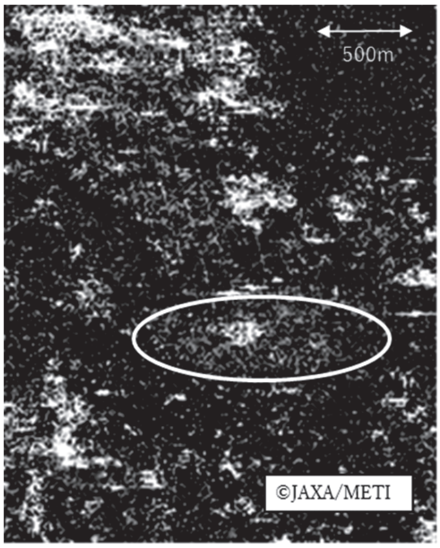

24^{th} August 2008

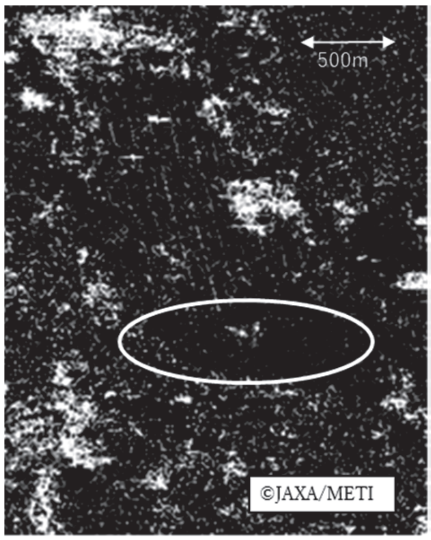

9^{th} October 2008

Fig. 8. Images of double bounce scatter component

result for a block cultivation area in which several paddy fields cultivated at the same time with the same crop appear as one unit.

Figure 9 shows the block scale and parcel scale polygons overlaid onto the image of the odd scatter components in the Freeman and Durden three-component decomposition analysis (upper left: parcel scale, upper right: block scale) and the scatter plots of the Odd and Dbl components (lower). Parcels are divided by ridges or foot paths; one parcel is one body of water. Blocks are divided by roads; one block contains multiple parcels. These scatter plots indicate that the block scale was able to achieve a more accurate classification than the parcel scale. The resolution of the fully polarimetric mode PALSAR observations is about 30 m, while typical Japanese paddy fields range between 10 a and 30 a. For example, a typical 30 a paddy field is 100 m by 30 m. Therefore, the resolution of the fully polarimetric mode PALSAR observation is insufficient for most Japanese paddy field parcels.

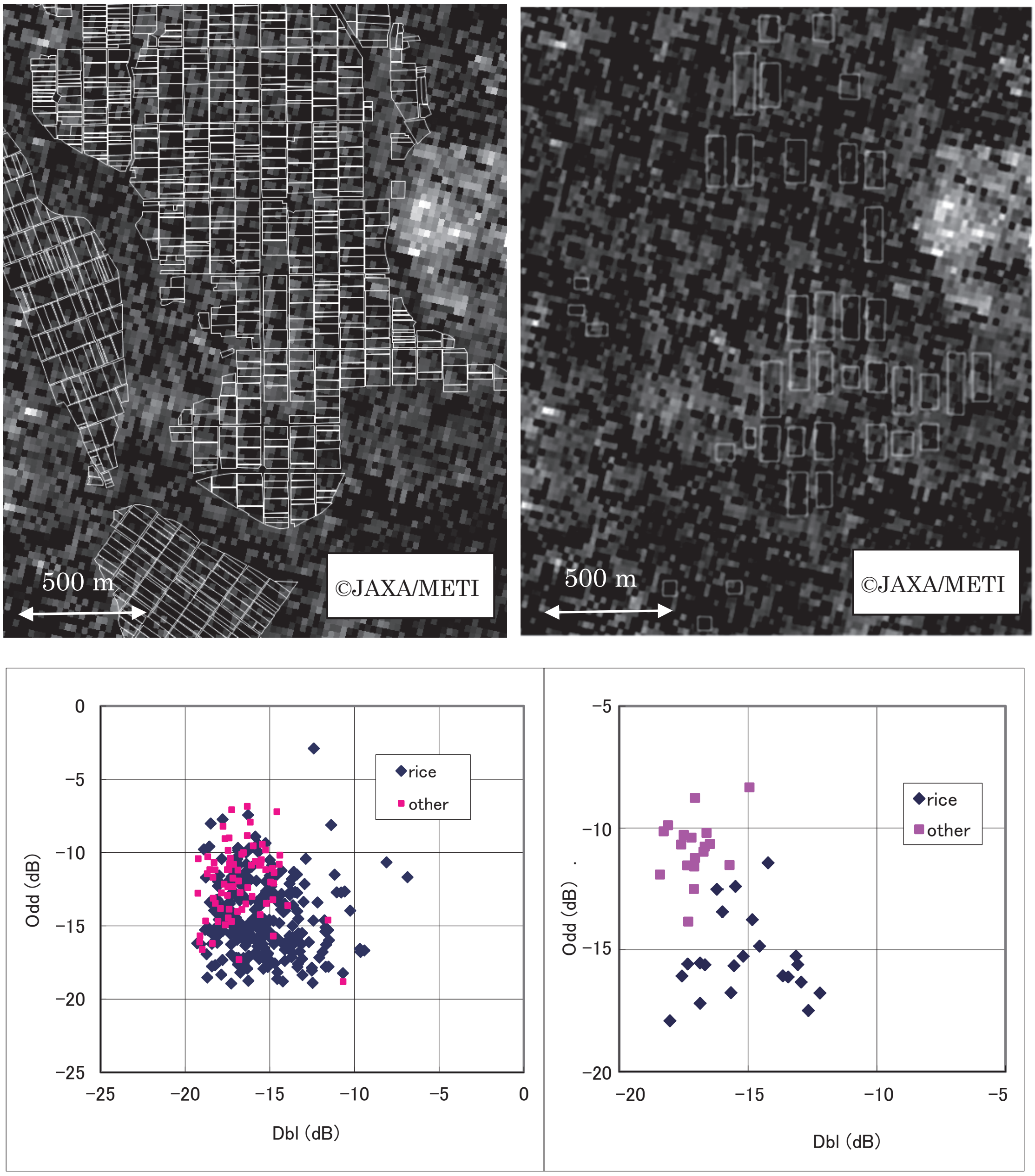

Fig. 9. Odd scatter component image of 24th August 2008 and scatter plot (left side: parcel scale, right side: block scale)

Conclusions

This paper has introduced several studies on area determination using SAR water surface detection. The author has demonstrated the suitability of SAR for applications in agriculture, flooding, water use, and the detection of paddies.

SAR can make observations during periods of cloud cover. This paper has shown that difficulties remain regarding the use of SAR for analysis, but this situation is improving as the number of SAR satellites increases, as more free software becomes available, and as SAR techniques improve, including the use of polarimetry and improvements in resolution.

References

Freeman, A. & Durden, S. L. (1998) A three-component scattering model for polarimetric SAR data. *IEEE Transactions on Geoscience and Remote Sensing*, **36**, 963-973

Ishitsuka, N. (2011) Observation of Japanese paddy fields using PALSAR data. Geoscience and Remote Sensing Symposium (IGARSS 2011).

Ishitsuka, N. (2013) Detection of paddy rice fields recovered from tsunami damage. ACRS2013.

Ishitsuka, N. (2014) Recover monitoring of paddy rice fields damaged by tsunami using SAR. Handbook of agricultural remote sensing enlarged edition, 242-243 [In Japanese].

Ishitsuka, N. (2015) The understanding of land cover situation on the farmland in 2011 using satellite data at Fukushima. *Bulletin of National Institute for Agro-Environmental Sciences*, **34**, 81-100 [In Japanese].

Ishitsuka, N. et al. (2003) Methodology Development for Area Determination of Rice Planted Paddy Using RADARSAT Data. *Journal of The Remote Sensing Society of Japan*, **23**(5), 458-472 [In Japanese].

JAXA, Polarimetric observation by PALSAR. http://www.eorc.jaxa.jp/ALOS/en/img_up /pal_polarization.htm.

Kurosu, T. et al (1995) Monitoring of rice crop growth from space using ERS-1 C-band SAR. *IEEE. Trans. Geosci. Remote Sensing*, **33**, 1092-1096.

Le Toan, T. et al. (1997) Rice crop mapping and monitoring using ERS-1 data based on experiment and modeling results. *IEEE Transactions on Geoscience and Remote Sensing*, **35**, 41-56.

McNairn, H. et al (2009) The Contribution of ALOS PALSAR Multipolarization and Polarimetric Data to Crop Classification. *IEEE Trans. on Geosci. Remote Sensing*, **47**(12), 3981-3992.

Ministry of Agriculture, Forestry and Fisheries (2010) Report on "The project for development of application using satellite images to measure paddy rice planted area in FY2009. unpublished and not for sale [In Japanese].

Okamoto, K. & Fukuhara, M. (1996) Estimation of paddy field area using the area ratio of categories in each mixel of Landsat TM. *International Journal of Remote Sensing*, **17**(9), 1735-1749.

Oki, T. & Kanae, S. (2004) Virtual water trade and world water resources. *Water Science & Technology*, **49**(7), 203-209.

Takata, Y. et al. (2014). Spatial prediction of radioactive Cs concentration in agricultural soil in eastern Japan (Environment). *Soil Science and Plant Nutrition*, **60**(3), 393-403.